

# Enhanced PWM Backscattering System for Battery-Free Wireless Sensors

Mahmoud H. Ouda<sup>1</sup>, Richard Penty<sup>2</sup>, Michael Crisp<sup>3</sup>

Centre for Photonic Systems, Department of Engineering,  
University of Cambridge, 9 JJ Thomson Avenue, Cambridge CB3 0FA, U.K.

<sup>1</sup>mhio2@cam.ac.uk, <sup>2</sup>rvp11@cam.ac.uk, <sup>3</sup>mjc87@cam.ac.uk

**Abstract**—Backscatter communication enables a passive long-range wireless link for low-power wireless sensors and Internet-of-things devices. In this paper, we propose encoding analog sensor data by PWM and a method to receive for wireless sensor readers to recover and decode the sensor data at lower power levels than conventional RFID readers, using commercial open-source software-defined radios. The high Rx sensitivity can be used to relax the minimum modulating voltage (and power) requirement from the sensor tag. Consequently, the wireless power sensitivity and the range of the sensor tag are extended. The proposed backscattering system is prototyped, and the proposed technique is verified to recover and decode PWM backscattered signals at low received RF power below -70dBm and with low modulation efficiency from a subthreshold backscatter modulator.

**Keywords**—Backscatter Communication, Battery free, Internet of Things, RFID, Sensors.

## I. INTRODUCTION

The Internet-of-things (IoT) demand for ever-lower power wireless sensors accelerates the research toward battery-free wireless micro-systems, advancing both the wireless powering and communication technologies [1], [2], [3]. The range of the wireless power link is mainly defined by the minimum RF power required by the rectenna to supply the minimum required voltage to run the sensor chip. Two ways to improve this sensitivity are to improve the rectenna RF-to-dc power conversion efficiency [4] or to reduce the minimum supply voltage required on the sensor chip by operating the sensor circuits in the subthreshold region [5], [6].

Most of RFID's and wireless sensors transmits the sensed data using digital modulations such as: ON-OFF Keying, or Frequency Shift Keying, which require an on-chip analog-to-digital converter, ADC, to convert the analog sensed signal. Recently, an analog pulse width modulation, PWM, is utilized in a battery-free wireless camera [7], to encode the raw analog signals directly from the pixels with no need for power-hungry on-chip ADC's. However, due to the self-leakage problem in the backscattering communication systems, the receiver picks up the strong transmitted RF signal. Hence, the received backscattered signal can be completely buried in the phase noise of the strong leaked carrier. As a remedy, a sub-carrier modulation step is added in [7] to up-convert the backscattered signal; however, it requires an extra XOR modulator and a high-frequency signal oscillator on the sensor chip. Since the modulator power is proportional to switching speed, this will also reduce the ultimate range.

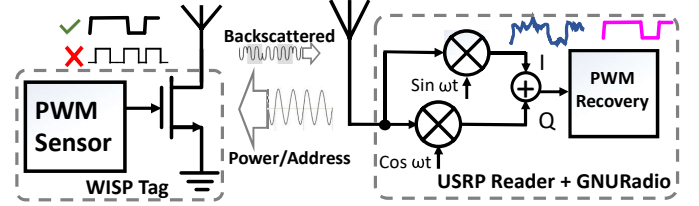


Fig. 1. The block diagram of backscattered PWM sensor and reader.

In this work, we propose an enhancement technique to improve the reader sensitivity so that there is no need to up-convert the PWM encoded signal. This saves all the power consumption of the ADC, the up-converting XOR/mixer and the extra VCO in the tag. Also, the proposed technique allows for lower modulation efficiency on the tag, which relaxes the required modulating voltage (and power) from the tag rectenna. Consequently, this improves the wireless power sensitivity of the tag and hence the wireless range. A backscattering PWM sensor system is depicted in Fig.1; the reader transmits power and address to the wireless identification and sensing platform (WISP) tag, which responds by backscattering the received signal, with the modulated PWM signal. The reader down-converts and sums the I and Q signals to recover the PWM signal.

## II. ENHANCED BACKSCATTERING WISP SYSTEM

### A. Backscattering Operation

Backscattering modulation is a passive technique for wireless communication, commonly used in RFID and low-power sensor systems, in which the tag (transponder) reflects a portion of the received carrier power back to the reader. Hence, the tag reuses the reader carrier power with no need for a RF local oscillator on the tag. The two states (high/low) of the tag binary data are encoded as a variation in the reflected power to the reader, by modulating the load impedance (and hence the reflection coefficient) of the tag antenna. A simple yet effective way to modulate the antenna load is achieved by a shunt transistor, as shown in Fig. 1.

The modulation efficiency is a higher function of the modulation factor ( $\Delta\Gamma$ ), defined as the difference between the reflection coefficients of the two modulated states,  $\Delta\Gamma = |\Gamma_1 - \Gamma_0|$ , where  $\Gamma_1$  and  $\Gamma_0$  are the reflection coefficients of the high and low states, respectively. Hence, the modulation efficiency increases by driving the transistor with a higher gate voltage,  $a_m$ . In order to characterize the modulation efficiency as a

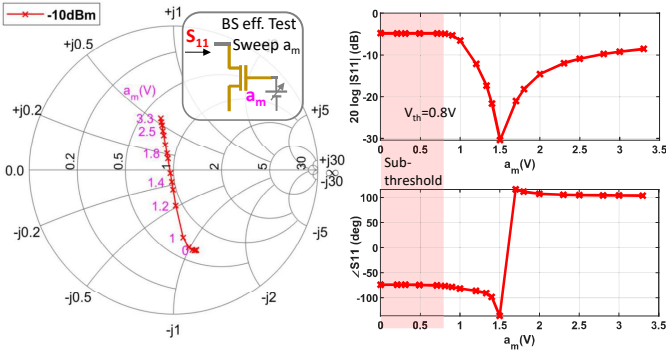


Fig. 2. The measured  $S_{11}$  of the backscattering transistor versus different backscatter voltages  $a_m$ .

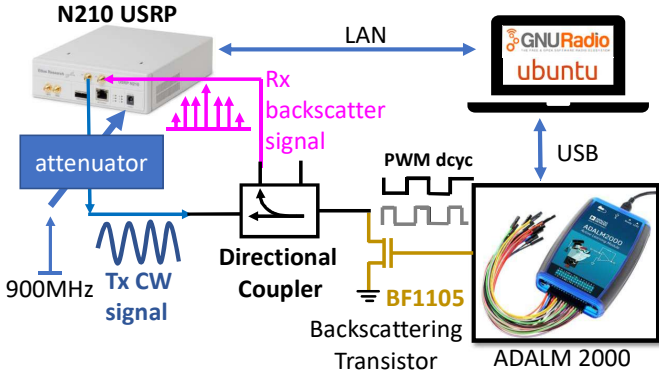


Fig. 3. The setup of the prototyped backscattering system.

function of the driving voltage,  $a_m$ , the transistor scattering parameter,  $S_{11}$ , is measured and plotted in Fig.2 versus the applied gate voltage,  $a_m$ , and over Smith Chart.

Obviously from Smith Chart, as  $a_m$  increases, the biased  $S_{11}$  moves far from its initial state ( $a_m = 0V$ ), and consequently the two modulating states become more distinguishable at the reader. However,  $a_m$  is limited by the tag rectified voltage and its rectenna RF sensitivity. Using a higher  $a_m$  drains the tag harvested energy sooner and limits the communication time. On the other hand, using small modulating signal,  $a_m$ , leads to a poor modulation efficiency and hence, a weak noisy PWM signal at the receiver.

### B. Backscattering System Prototype and Setup

In order to emulate the proposed concept, a backscattering prototype setup is built, as shown in Fig.3. The USRP N210 software-defined radio is used, as a reader, to send a UHF 900MHz continuous wave (CW) to the backscattering transistor, through a variable attenuator. The WISP tag is emulated by the BF1105 transistor modulated by a PWM signal generated from the Analog Devices (ADALM2000). The backscattered PWM signal travels, through a directional coupler (with coupling=-10dB), back to the reader (USRP N210). Then, the received backscattered signal is downconverted into the complex (I, Q) streams which are summed together to extract the raw PWM signal. Both the ADALM2000 backscattering PWM driver and the USRP reader are controlled in the GNURadio software [8].

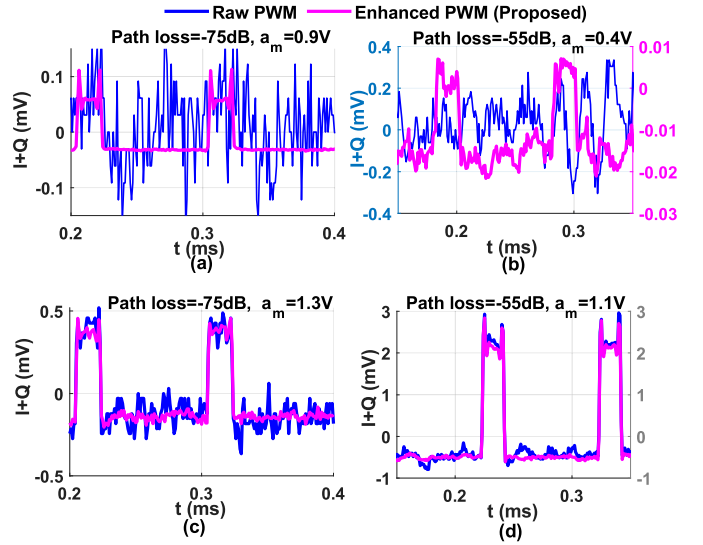


Fig. 4. The downconverted backscattered signals, I+Q, (before and after) the proposed technique using the minimum backscatter voltage  $a_m$  required for the proposed technique at path loss (a) -75dB (b) -55dB, and using the minimum  $a_m$  required for the direct method at the same loss (c) and (d) .

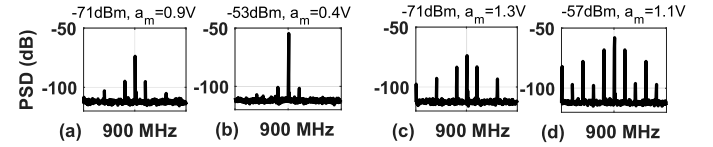


Fig. 5. The backscattered RF spectrum of the four cases of minimum  $a_m$  for the proposed at path loss (a) -75dB (b) -55dB, and for the direct method at the same loss (c) and (d).

### C. PWM Signal Recovery and Decoding

A direct method to decode the received PWM signal is to remove the dc component, and apply a squarer to restore the PWM signal, then measure the pulse width,  $t_{pw}$ , and duty cycle,  $dcyc$ . Given that, the sensor signal is much slower than the read sample rate (i.e. the PWM frequency), the accuracy could be improved by averaging the measured  $dcyc$  of multiple PWM cycles over time. However, the individual PWM cycles are already received weak and noisy, due to either a low received carrier power,  $P_{Rx}$ , as shown in Fig. 4a and 5a, or due to a low modulation efficiency (i.e. small  $a_m$ , and low sidebands), as shown in Fig. 4b and 5b. Hence, these raw PWM pulses can not be restored by a squarer or time averaging.

### D. Enhanced PWM Signal Recovery Technique

In this study, we propose an enhancement technique to recover the downconverted PWM signal, by converting segments of few (3-to-5) PWM cycles into frequency domain, by applying FFT over each segment, then averaging the FFT's of the segments, and returning to time domain using iFFT. The proposed technique recovers the PWM signal at low power level, such as  $P_{Rx} = -71dBm$ , and at low modulation efficiency,  $a_m = 0.4V$ , as shown in Fig. 4a, and 4b, respectively. On the contrary, the direct technique is not able to recover the PWM signal, at the same power level, shown in Fig.4a, until

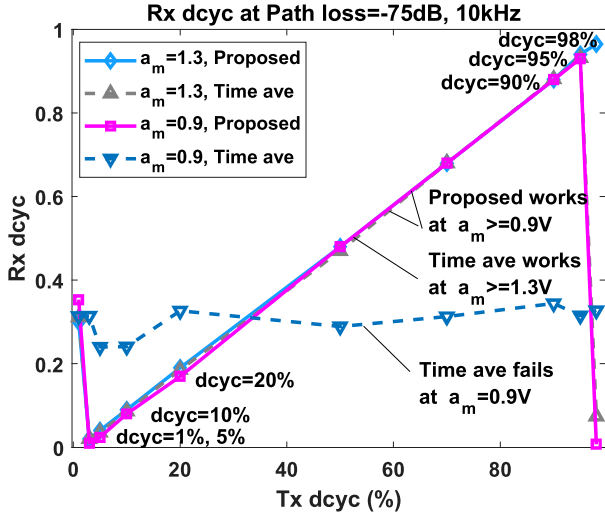


Fig. 6. The measured duty cycles of the received  $I + Q$  for the proposed and the time averaged techniques both at their minimum backscatter voltages  $a_m = 0.9$  and  $1.3$ , at path loss=-75dB and  $P_{Rx} = -71$ dBm

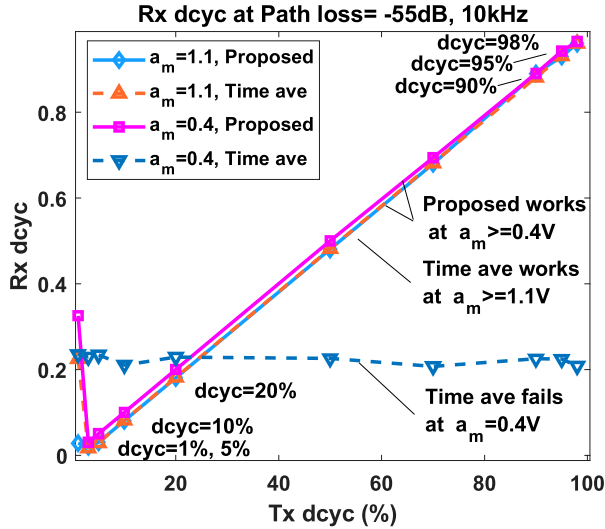


Fig. 7. The measured duty cycles of the received  $I + Q$  for the proposed and the time averaged techniques both at their minimum backscatter voltages  $a_m = 0.4$  and  $1.1$ , at pathloss=-55 dB and  $P_{Rx}$  around -53dBm.

the modulation efficiency is increased to  $a_m = 1.3$ V, as shown in Fig. 4c. Even at higher power level,  $P_{Rx} = -53$ dBm (path loss= -55dB), shown in Fig.4b, the direct technique fails to recover the PWM signal, at the same modulation  $a_m = 0.4$ V until increased to  $a_m = 1.1$ V, shown in Fig.4d.

### III. RESULTS AND DISCUSSION

In order to fully test and compare the proposed and direct techniques, the  $dcyc$ , representing the sensor output value, is swept from 1%, 5%, and 10% to 90%, 95% and 98%, and the  $a_m$ , representing the modulation efficiency, is swept from 0.1 to 3V. The recovered Rx  $dcyc$ 's using both techniques are plotted in Fig.6, at path loss=-75dB ( $P_{Rx} = -71$ dBm), for the minimum successful  $a_m$  values for each technique.

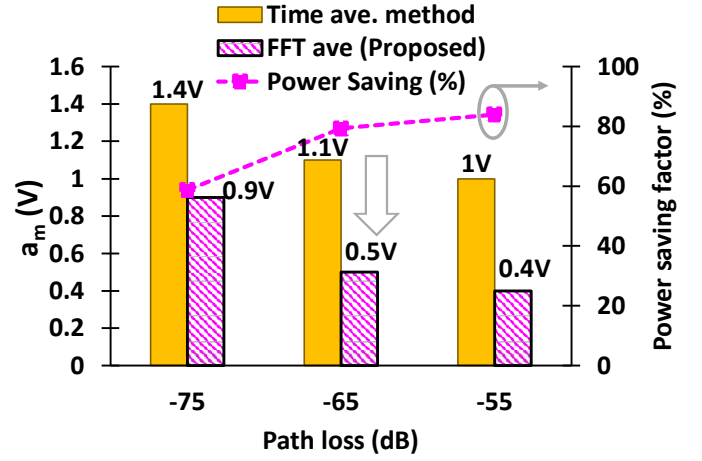


Fig. 8. The minimum backscatter voltages  $a_m$  for detecting the PWM signal with the time average and proposed techniques (left), and the power saving percentage due to the scaling down of  $a_m$  (right) versus path loss.

As shown in Fig.6, the proposed technique recovers small  $dcyc$  as 5% with a low  $a_m = 0.9$ V, while the direct time averaging fails to recover the  $dcyc$  until the  $a_m$  increased to 1.3V. Repeating the same experiment at higher  $P_{Rx} = -53$ dBm, which is expected for a 3m distance, the proposed technique successfully recovers fine Rx  $dcyc$ , such as 98% with a very low  $a_m = 0.4$ V (i.e. low modulation efficiency), while the direct time averaging method fails until  $a_m$  is increased to 1.1V. As a result of  $a_m$  scaled down, the tag power consumed in the PWM sensor, comparator, and voltage controlled oscillator are all scaled down roughly by  $a_m^2$ . A power saving factor is calculated as the percentage by which  $a_m^2$  (and hence the power) is reduced. The scaling of minimum  $a_m$  required for both techniques at path loss=-75, -65 and -55 dB, alongside with the tag power saving factor are plotted in Fig.8. A significant power saving of 60-to-85% can be achieved using the proposed technique relative to the time averaging method.

### IV. CONCLUSION

This paper presented a brief study for PWM backscattering system and proposed an enhancement technique to recover and decode the PWM backscattered signals at low power below -70dBm and low modulation efficiency of sub-threshold backscattering modulator. The prototyped system is presented and the backscattering modulator is characterised versus different modulating voltage signals. The proposed enhancement technique is verified over wide scale of duty cycles and modulation efficiency and the system performance limits are extended and highlighted.

### ACKNOWLEDGMENT

This work was supported by EPSRC EP/S-19405/1 Channel Optimised Distributed Passive Sensor Networks.

### REFERENCES

- [1] C. Sutardja and J. M. Rabaey, "Isolator-Less Near-Field RFID Reader for Sub-Cranial Powering/Data Link of Millimeter-Sized Implants," *IEEE Journal of Solid-State Circuits*, vol. 53, no. 7, pp. 2032-2042, 2018.

- [2] J. F. Ensworth and M. S. Reynolds, "BLE-Backscatter: Ultralow-Power IoT Nodes Compatible With Bluetooth 4.0 Low Energy (BLE) Smartphones and Tablets," *IEEE Transactions on Microwave Theory and Techniques*, vol. 65, no. 9, pp. 3360–3368, 2017.
- [3] S. Daskalakis, J. Kimionis, A. Collado, M. M. Tentzeris, and A. Georgiadis, "Ambient FM backscattering for smart agricultural monitoring," in *2017 IEEE MTT-S International Microwave Symposium (IMS)*, 2017, pp. 1339–1341.
- [4] M. H. Ouda, W. Khalil, and K. N. Salama, "Wide-Range Adaptive RF-to-DC Power Converter for UHF RFIDs," *IEEE Microwave and Wireless Components Letters*, vol. 26, no. 8, pp. 634–636, 2016.
- [5] I. Lee, D. Sylvester, and D. Blaauw, "A subthreshold voltage reference with scalable output voltage for low-power iot systems," *IEEE Journal of Solid-State Circuits*, vol. 52, no. 5, pp. 1443–1449, 2017.
- [6] K. Yang, Q. Dong, W. Jung, Y. Zhang, M. Choi, D. Blaauw, and D. Sylvester, "9.2 A 0.6nJ  $-0.22/+0.19^{\circ}\text{C}$  inaccuracy temperature sensor using exponential subthreshold oscillation dependence," in *2017 IEEE International Solid-State Circuits Conference (ISSCC)*, 2017, pp. 160–161.
- [7] A. Saffari, M. Hesar, S. Naderiparizi, and J. R. Smith, "Battery-Free Wireless Video Streaming Camera System," in *2019 IEEE International Conference on RFID (RFID)*, 2019, pp. 1–8.
- [8] G. Radio, *The free open software radio ecosystem*, 2020. [Online]. Available: <http://gnuradio.org>